ORIGINAL RESEARCH

Variant R94C in *TNNT2*-Encoded Troponin T Predisposes to Pediatric Restrictive Cardiomyopathy and Sudden Death Through Impaired Thin Filament Relaxation Resulting in Myocardial Diastolic Dysfunction

Jordan E. Ezekian, MD, MPH;* Sarah R. Clippinger;* Jaquelin M. Garcia; Qixin Yang, MD; Susan Denfield, MD; Aamir Jeewa, MD; William J. Dreyer, MD; Wenxin Zou, PhD; Yuxin Fan, MD; Hugh D. Allen, MD; Jeffrey J. Kim, MD; Michael J. Greenberg, PhD; Andrew P. Landstrom, MD, PhD

***Background*—**Pediatric-onset restrictive cardiomyopathy (RCM) is associated with high mortality, but underlying mechanisms of disease are under investigated. RCM-associated diastolic dysfunction secondary to variants in *TNNT2*-encoded cardiac troponin T (TNNT2) is poorly described.

***Methods and Results*—**Genetic analysis of a proband and kindred with RCM identified TNNT2-R94C, which cosegregated in a family with 2 generations of RCM, ventricular arrhythmias, and sudden death. TNNT2-R94C was absent among large, population-based cohorts Genome Aggregation Database (gnomAD) and predicted to be pathologic by in silico modeling. Biophysical experiments using recombinant human TNNT2-R94C demonstrated impaired cardiac regulation at the molecular level attributed to reduced calcium-dependent blocking of myosin's interaction with the thin filament. Computational modeling predicted a shift in the force-calcium curve for the R94C mutant toward submaximal calcium activation compared within the wild type, suggesting low levels of muscle activation even at resting calcium concentrations and hypercontractility following activation by calcium.

***Conclusions*—**The pathogenic TNNT2-R94C variant activates thin-filament–mediated sarcomeric contraction at submaximal calcium concentrations, likely resulting in increased muscle tension during diastole and hypercontractility during systole. This describes the proximal biophysical mechanism for development of RCM in this family. **(*J Am Heart Assoc*. 2020;9:e015111. DOI: 10.1161/JAHA.119.015111.)**

Key Words: heart failure • myocardial biology • pediatrics • restrictive cardiomyopathy • sudden cardiac death

Restrictive cardiomyopathy (RCM) is a primary disorder of increased myocardial stiffness and diastolic dysfunction with often normal to slightly hypertrophied ventricular wall thickness.[1] This disease typically manifests with marked atrial dilation, attributable to transmission of elevated pressures during ventricular relaxation, with preserved ventricular systolic function. The etiologies of RCM are broad, including inherited and acquired causes, and the prognosis is poor.[2,3]

RCM comprises one of a group of primary muscle diseases of the heart collectively called cardiomyopathies. Once thought to be separate entities, cardiomyopathies are now thought to be a spectrum of diseases with the presence of restrictive and hypertrophic features varying across the phenotypes. Hypertrophic cardiomyopathy (HCM) is common and is associated with mutations in sarcomere protein-encoding genes.[4–7] RCM and HCM patients often share the feature of diastolic

From the Division of Pediatric Cardiology, Departments of Pediatrics (J.E.E., Q.Y., A.P.L.) and Cell Biology (A.P.L.), Duke University School of Medicine, Durham, NC; Department of Biochemistry and Molecular Biophysics, Washington University in St. Louis, St. Louis, MO (S.R.C., J.M.G., M.J.G.); Department of Peadiatrics, The Lillie Frank Abercrombie Section of Pediatric Cardiology, Baylor College of Medicine, Houston, TX (S.D., W.J.D., W.Z., Y.F., H.D.A., J.J.K.); Department of Paediatrics, The Hospital for Sick Children, Toronto, Ontario, Canada (A.J.).

An accompanying Table S1 is available at https://www.ahajournals.org/doi/suppl/10.1161/JAHA.119.015111

*Dr Ezekian and Ms Clippinger contributed equally to this work and are co-first authors.

Correspondence to: Michael J. Greenberg, PhD, Department of Biochemistry and Molecular Biophysics, Washington University School of Medicine, 660 S Euclid Ave, Campus Box 8231, St. Louis, MO 63110. E-mail: greenberg@wustl.edu and Andrew P. Landstrom, MD, PhD, Duke University School of Medicine, Duke University Medical Center, Box 2652, Durham, NC 27710. E-mail: andrew.landstrom@duke.edu

Received November 12, 2019; accepted January 17, 2020.

Clinical Perspective

What Is New?

- *TNNT2*-encoded cardiac troponin T TNNT2-R94C is a heritable cause of restrictive cardiomyopathy and sudden death.
- This pathologic variant leads to initiation of cardiac muscle contraction at resting calcium levels.
- Computational modeling predicts that this causes increased basal muscle tension and likely leads to diastolic cardiac dysfunction.

What Are the Clinical Implications?

- Pediatric restrictive cardiomyopathy is a rare cause of sudden cardiac death in children.
- This study demonstrates the pathological mechanism of the TNNT2-R94C variant.
- Patients with this variant should be followed closely for development of cardiomyopathy and/or arrhythmias, and familial screening should be performed when the variant is discovered in an individual.

dysfunction, and a subset of patients with RCM demonstrate mild ventricular hypertrophy. The genetic mechanisms underlying RCM, corresponding clinical phenotypes, and subclass of RCM with hypertrophic features have not been well described.

To date, >1000 variants associated with cardiomyopathy have been identified in sarcomeric genes, including *TNNT2*-encoded cardiac troponin T (TNNT2).[7,8] TNNT2 combines with the calcium-binding proteins troponin C and troponin I to form the troponin complex. This troponin complex is integrated into the thin filament of the sarcomere and, in combination with tropomyosin, coordinates contraction of the cardiac muscle by regulating the calcium-dependent interaction between myosin and the thin filament. *TNNT2*-specific gene variants are a known, rare cause of HCM, found in 3% to 5% of patients with HCM.[9] They have also been associated with the development of ventricular arrhythmias.[10–13] Recent studies have suggested that variants in *TNNT2* may also be associated with development of RCM.[14–16] For example, the TNNT2 variant, I79N, has been shown to cause RCM and HCM within the same family.[17] Previous biochemical studies have suggested that *TNNT2* variants identified in patients with HCM and dilated cardiomyopathy result in alterations in calcium sensitivity, leading to systolic dysfunction.[18,19] Based on these findings, this molecular mechanism has been extrapolated to disorders of diastolic dysfunction. To confirm this hypothesis, variants known to produce a clinical phenotype of primary diastolic dysfunction and RCM should be studied to confirm the underlying molecular mechanisms.

Herein, we identify a *TNNT2* variant, TNNT2-R94C, in a family with multiple members affected with a range of clinical presentations, including arrhythmias, cardiomyopathy with predominantly restrictive physiology, and sudden death. We used biochemical techniques and computational modeling to demonstrate that this variant is likely pathogenic, and we determined its molecular mechanism. We show that this variant causes activation of the thin filament at submaximal calcium concentrations, contributing to diastolic dysfunction as observed in this family.

Methods

The data that support the findings of this study are available from the corresponding author upon reasonable request.

Clinical Evaluation

This study received approval from the institutional review boards at Baylor College of Medicine and Duke University Health System. Available clinical data from the identified proband and relatives were collected, which included pertinent personal and family history, physical examination, standard 12-lead ECG analysis, echocardiographic testing, cardiac catheterization data, and genetic testing. An autopsy was performed on the brother of the proband by the Medical Examiner Service of the Harris County, Texas, Institute of Forensic Sciences (Houston, TX) following his death. The family underwent a full evaluation by pediatric cardiomyopathy and heart failure specialists.

Genetic Analysis

The proband underwent clinical genetic testing using the Famillion (New Haven, CT) HCM panel test, which involves sequencing 9 sarcomeric genes (*ACTC*, *MYBPC3*, *MYH7*, *MYL2*, *MYL3*, *TNNT2*, *TNNI3*, *TNNC1*, and *TPM1*) and 3 metabolic genes (*GLA*, *LAMP2*, and *PRKAG2*). Clinical genetic testing was performed on family members using the same HCM panel test. Subsequently, Sanger sequencing was utilized for confirmatory testing. For this, genomic DNA was isolated using the Gentra Puregene Blood Kit (Qiagen, Valencia, CA) from peripheral whole blood as well as postmortem blood spot. To confirm the absence of the identified presumed pathogenic variant in ostensibly healthy individuals, the publicly available Genome Aggregation Database (gnomAD) was used as a control cohort, which is comprised of a total of 15 708 genomes and 125 748 exomes from 141 456 individuals.[20] Though the gnomAD database is comprised partly of various disease-specific cohorts in addition to population genetics studies, it excludes individuals known to have severe pediatric disease or severe disease in their first-degree relatives. These individuals were therefore utilized as "control" or "reference" alleles. Variant

pathogenicity classification was also assigned based on 2015 American College of Medical Genetics criteria[21] and ClinVar (National Center for Biotechnology Information).[22]

Sequencing Conservation

Sequence conservation analysis was performed using the primary TNNT2 sequence obtained from the National Center for Biotechnology Information (NP_001001430.1).[23] Multalign alignment algorithms were utilized to determine sequence conservation across species.[24,25]

In Silico Variant Pathogenicity Modeling

In silico variant pathogenicity prediction was performed using GenMAPP,[26] PolyPhen-2,[27] PredictSNP,[28] SIFT,[29] SNAP,[30] and PANTHER[31] prediction tools. Variants were considered pathogenic if they carried the designation of "damaging or probably damaging," "deleterious," "disease-related," and/or "disease-associated." Variants were considered benign if they carried designation of "tolerated," "benign," or "neutral."

Purification of Cardiac Myosin and Actin

Porcine cardiac ventricular myosin and actin were purified from cryoground tissue as previously described.[32–34] Myosin subfragment 1 was prepared by chymotrypsic digestion as previously described,[32] using standard techniques,[35,36] and the purity of the protein was assessed by SDS-PAGE. The concentration of myosin subfragment 1 was determined by absorbance at 280 and 320 nm. Pyrene-labeled actin was prepared from acetone powder[37] and labeled with the dye, N-(1-pyrenyl)iodoacetamide (pyrene), as described previously.[38,39] Concentration of pyrene actin was determined by absorbance at 290 and 344 nm. Before use, all actin was stabilized by incubating with equimolar concentrations of phalloidin.

Preparation of Recombinant Human Troponin and Tropomyosin

Human cardiac tropomyosin was expressed in BL21-CodonPlus cells (Agilent Technologies, Santa Clara, CA) and purified using established protocols.[32,33,40,41] On the day of the experiment, tropomyosin was reduced in 50 mmol/L of DTT at 56°C for 5 minutes, and aggregates were subsequently removed by ultracentrifugation at 436 000*g* in an Optima MAX-TL Ultracentrifuge (Beckman Coulter, Brea, CA).[42] The R94C variant was introduced into *TNNT2* using the QuickChange Site-Directed Mutagenesis kit (Agilent Technologies). Human troponins I, T, and C were expressed in BL21-CodonPlus cells (Agilent Technologies), purified, and complexed using established protocols.[43]

Determination of K_B Using Stopped Flow Transient Kinetics

To determine the equilibrium constant between the blocked and closed states, K_B, a stopped flow approach developed by McKillop and Geeves[32,44] was utilized. This method analyzes the rate of myosin binding to reconstituted thin filaments in the presence and absence of calcium. Pyrene-actin was excited at 365 nm, and fluorescence emission was detected using a 390 nm long-pass filter. Reconstituted thin filaments (5 μmol/L of phalloidin-stabilized pyrene actin, 2 μmol/L of tropomyosin, and 2 μmol/L of troponin) and 0.04 U/mL of apyrase were rapidly mixed with 0.5 μmol/L of subfragment 1 myosin and 0.04 U/mL of apyrase at 20°C in an SX-20 stopped flow apparatus (Applied Photophysics, Leatherhead, UK). The high calcium (pCa 4) buffer contained 200 mmol/L of KCl, 5 mmol/L of $MgCl_2$, 60 mmol/L of MOPS, 2 mmol/L of EGTA, 1 mmol/L of DTT, and 2.15 mmol/L of $CaCl_2$. The low calcium (pCa 9) buffer contained 200 mmol/L of KCl, 5 mmol/L of $MgCl_2$, 60 mmol/L of MOPS, 2 mmol/L of EGTA, 1 mmol/L of DTT, and 5.2 μmol/L of $CaCl_2$. Myosin strong binding to pyrene-labeled actin in reconstituted thin filaments quenches pyrene fluorescence. Fluorescence transients were collected for at least 3 separate mixes, and a single exponential function was fit to the transient. K_B is calculated from the ratio of the rates of myosin binding to the reconstituted thin filaments at high and low calcium[44]:

$$\frac{k_{obs}(-Ca^{2+})}{k_{obs}(+Ca^{2+})} \approx \frac{K_B}{1+K_B} \quad (1)$$

The average K_B was calculated from 3 different experiments, and the *P* value was calculated from a 2-tailed Student *t* test.

Determination of K_W, K_T, and *n* From Fluorescence Titrations

Values of the equilibrium constant between the open and weakly bound myosin states, K_W, the equilibrium constant between the closed and open states K_T, and the size of the cooperative unit (ie, the number of binding sites on the thin filament opened by myosin binding), *n*, were determined by measuring the steady-state binding of myosin to pyrene-labeled regulated thin filaments.[44] Fluorescence titrations were carried out at 20°C in an Applied Photophysics SX-20. Myosin S1 was added at 1-minute intervals to a stirred cuvette containing 0.5 μmol/L of pyrene-actin, 0.27 μmol/L of troponin, and tropomyosin up to a final concentration of 10 μmol/L of

subfragment 1. Buffers contained 200 mmol/L of KCl, 5 mmol/L of free $MgCl_2$, 60 mmol/L of MOPS, 2 mmol/L of EGTA, 1 mmol/L of DTT, and 2 mmol/L of ADP and the desired free concentration of free calcium. Any contaminating ATP was eliminated by adding 50 μmol/L of P1,P5-di(adenosine-5′) pentaphosphate, 2 mmol/L of glucose, and 1 μmol/L of hexokinase. Titrations were performed at 3 calcium concentrations: low (2 mmol/L of EGTA), intermediate (pCa 6.25), and high (pCa 3). Five technical replicates were performed. Data was analyzed as previously described.[32]

To quantify differences in myosin binding of the wild-type (WT) and mutant proteins, titration curves were fit to the fractional change in the fluorescence, *a*, as a function of myosin, [*M*], given by:

$$a = \frac{F_0 - F}{F_0 - F_\infty} = \frac{K_W[M]P^{n-1}(K_T(1+K_S)^n+1)}{\left(K_T P^n + Q^n + \frac{1}{K_B}\right)(1+K_S)^{n-1}} \quad (2)$$

where *F* is the measured fluorescence, F_0 is the fluorescence of the pyrene in the absence of myosin binding, F_∞ is the fluorescence at saturating myosin concentrations, *n* is the size of the cooperative unit, $P=1+K_W[M](1+K_S)$, and $Q=1+K_W[M]$.[44] For the fitting, the equilibrium constant between the closed and open states (K_T), the equilibrium constant between the open and myosin weakly bound state (K_W), and *n* were fitted parameters. Titration curves were globally fit to extract parameter values, 95% CIs by bootstrapping simulations, and *P* values were determined as described.[32] K_B was fixed based on stopped flow experiments. The equilibrium constant between the states in which myosin is weakly and strongly bound to the thin filament (K_S) was fixed based on previous studies.[45]

Computational Modeling of the Variants on Thin Filament Regulation

To quantitatively model the impacts of the variant on overall calcium-force production relationship in the heart, we utilized a computational model developed by the McCulloch laboratory, which uses the measured equilibrium constants to calculate the expected force per sarcomere as a function of calcium.[46] Model parameters for the mutant protein were adjusted to be proportional to our measured parameters, and we used these parameters to simulate a force-calcium curve. For the WT protein, we used the default model parameters.

Statistical Analysis

A Student *t* test was performed to determine statistical significance between 2 groups. $P<0.05$ was considered significant, unless otherwise noted.

Results

Clinical Evaluation

The proband is a 2-year-old white girl who was found to have RCM following an evaluation precipitated by the sudden death of her older brother. Her ECG demonstrated criteria for right and left atrial enlargement with marked repolarization abnormality. Echocardiogram revealed mild right atrial and severe left atrial enlargement (left atrial volume, 61.5 cc/m^2; normal, 16–28), with mildly increased left ventricular mass and otherwise normal ventricular dimensions. Right and left ventricular systolic function was preserved. These findings were consistent with a mild form of HCM with markedly restrictive physiology (Figure 1A and 1B). The proband suffered a cardiac arrest during phlebotomy and was unable to be resuscitated.

Her seemingly healthy 4-year-old brother presented with a sudden cardiac arrest while running on a soccer field and could not be resuscitated. Autopsy revealed mild cardiomegaly (heart weighed 147 g; normal, 55–121) with mild biventricular hypertrophy (left ventricular free wall 0.8 cm (echocardiographic Z-Score, +3.53), interventricular septum 0.9 cm (echocardiographic Z-Score, +4.78), and right ventricular free wall (0.3 cm) with myocyte hypertrophy and disarray found on histopathological examination.[47,48] These findings were determined to be consistent with a diagnosis of HCM, which was identified as the cause of death. Significant left ventricular outflow tract obstruction was not present. No genetic testing was performed at the time of death. Because of this diagnosis, clinical evaluation of the family was conducted, which included phenotypic screening and genetic testing.

The proband's father is a 35-year-old male who was found to have episodes of asymptomatic, nonsustained ventricular tachycardia and premature ventricular beats on event monitoring in the setting of normal biventricular size and systolic function. Cardiac magnetic resonance imaging demonstrated normal myocardium and marked right and left atrial enlargement, consistent with diastolic dysfunction and RCM (Figure, 1C through 1E).

Genetic Evaluation

Cardiomyopathy-based panel testing (Familion; Transgenomic, Inc., New Haven, CT) was conducted on the proband, demonstrating a single, heterozygous, variant TNNT2-R94C (c.280C>T). No other variants were identified in other cardiomyopathy-associated genes. This variant was absent in gnomAD and localized to a highly conserved portion of the N-terminal domain near the tropomyosin binding site (Figure 2A and 2B). To test whether this variant was found among all affected individuals, family history was expanded, and a

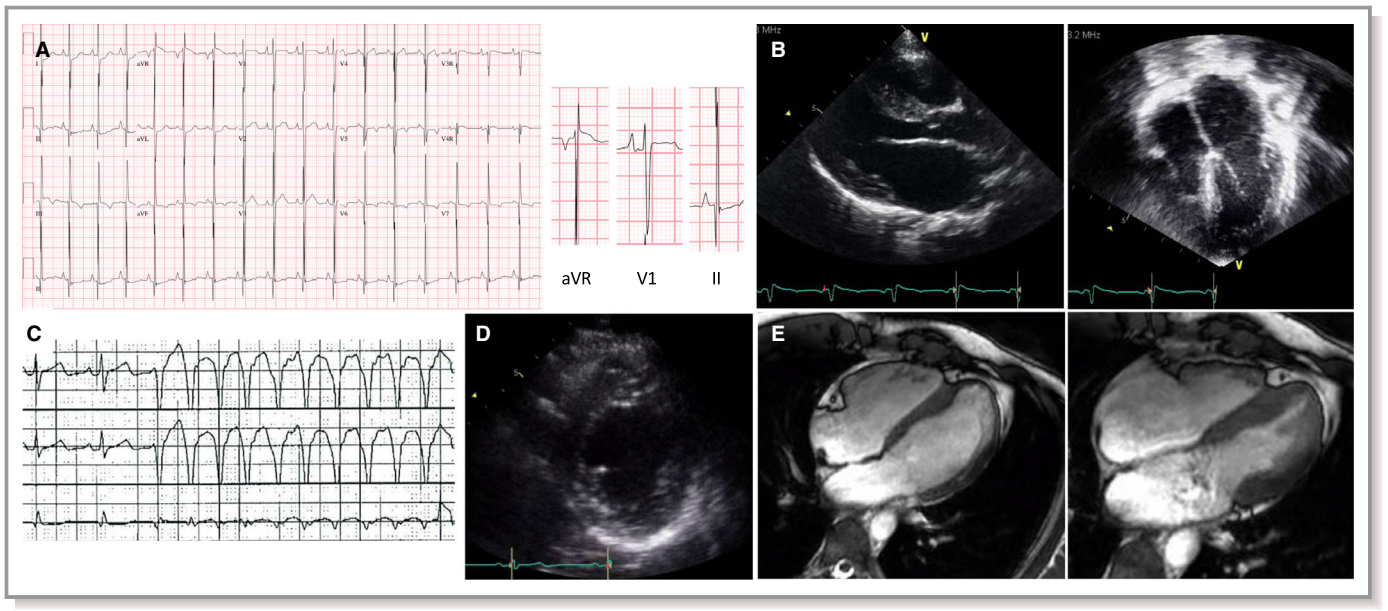

Figure 1. Clinical evaluation of TNNT2-R94C–positive kindred. (**A**) Representative ECG obtained from the proband demonstrating right and left atrial enlargement with nonspecific ST and T-wave abnormalities and ST depression in the inferolateral leads. An enlarged representative ECG is shown. (**B**) Representative echocardiographic images in the parasternal long axis and apical 4-chamber windows demonstrating severe left atrial enlargement. (**C**) Cardiac telemetry demonstrating ventricular tachycardia overtaking sinus rhythm. (**D**) Representative echocardiographic images from the father of the proband in the parasternal short-axis view demonstrating normal LV size and systolic function. (**E**) Representative cardiac MRI images demonstrating right and left atrial enlargement with normal biventricular size and function. LV indicates left ventricular; MRI, magnetic resonance imaging; TNNT2, *TNNT2*-encoded cardiac troponin T.

total of 8 kindred were consented and subjected for confirmatory genetic testing. In addition to the proband (IV.3), postmortem genetic testing of the deceased brother (IV.2) also demonstrated presence of the heterozygous TNNT2-R94C variant. While a first trimester fetal death (IV.4) was also identified from the mother (III.4), no fetal tissue was available for genetic analysis. The father (III.3) was also found to carry the TNNT2-R94C, which was absent in both paternal grandparents (II.1 and II.2) and paternal sibling (III.2), suggesting a de novo variant that was subsequently passed in an autosomal-dominant fashion. This is summarized in Figure 3. In silico prediction modeling was performed and demonstrated a prediction of deleterious impact from 5 of 6 models and neutral from 1 model, with an average confidence of 74.6% (Tabl). This variant was designated as pathologic in ClinVar, and there is strong evidence of pathogenicity based on 2015 American College of Medical Genetics criteria[21] for classifying pathogenic variants.

R94C Destabilizes the Blocked State of Tropomyosin and Increases the Equilibrium Constant for Myosin Weak Binding to the Thin Filament

Cardiac troponin T is part of the machinery that regulates the calcium-dependent interactions between myosin and the thin filament (Figure 4A). To determine the molecular consequences of the TNNT2-R94C variant on cardiac contractile regulation, we expressed human WT ($TNNT2^{WT}$) and mutant troponin ($TNNT2^{R94C}$) and determined the biochemical impacts on thin filament regulation.

The first step in muscle activation is the calcium-induced change in positioning of tropomyosin along the thin filament, moving it from the blocked to the closed state. The equilibrium constant that defines this transition, K_B, was calculated by measuring the rate of myosin binding to reconstituted thin filaments containing pyrene-labeled actin at high- and low-calcium concentrations.[32,44] The pyrene fluorescence is quenched upon myosin binding, and the rate of myosin binding to the thin filament can be calculated by fitting an exponential function to the fluorescence transient (Figure 4B). In $TNNT2^{WT}$, the rate of binding at high calcium (pCa 4) is faster than at low calcium (pCa 9) given that the blocked state is scarcely populated at high calcium. Whereas the fluorescence transients collected at high calcium are similar for the $TNNT2^{WT}$ and $TNNT2^{R94C}$, at low calcium, $TNNT2^{R94C}$ binds faster than the $TNNT2^{WT}$, consistent with less inhibition at low calcium in $TNNT2^{R49C}$. Consistent with this notion, we found that K_B for $TNNT2^{R94C}$ (0.67 ± 0.17) is significantly larger than K_B for the WT (0.40 ± 0.15; $P=0.04$). This result demonstrates that the inhibitory blocked state is less populated in $TNNT2^{R94C}$ at low calcium compared with

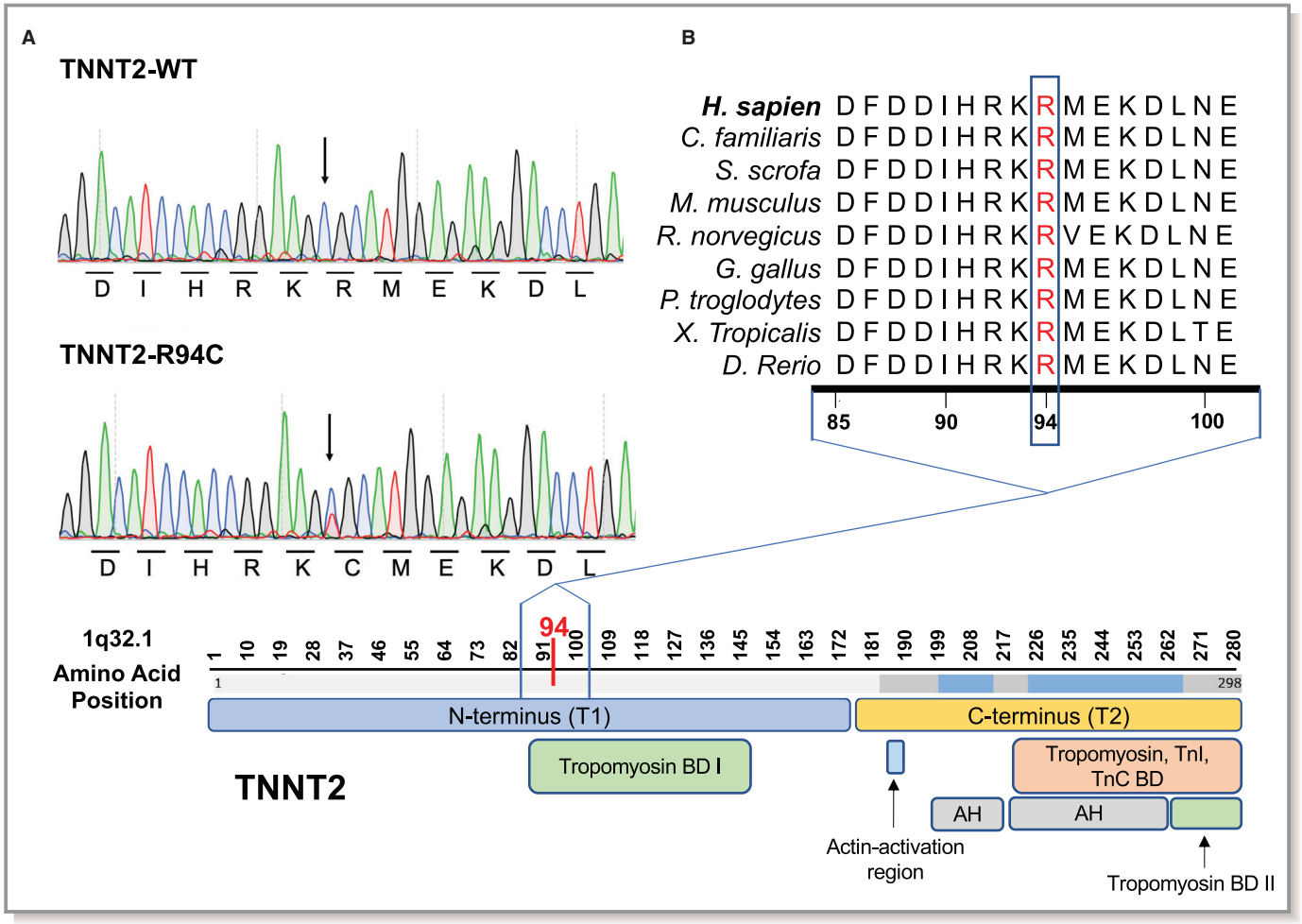

Figure 2. R94C localizes to a highly conserved region of TNNT2. (**A**) Sanger sequencing chromatograms of heterozygous mutant TNNT2-R94C (obtained from subject III-3) and wild-type genotypes. (**B**) The topological map of TNNT2 with primary sequence alignment from multiple divergent species is shown. The variant localizes to the N-terminal segment of TNNT2 in the tropomyosin binding domain I. This region is highly conserved across species. AH indicates actin helix; BD, binding domain; TnC, troponin C; TnI, troponin I; TNNT2, *TNNT2*-encoded cardiac troponin T; WT, wild type.

the $TNNT2^{WT}$. This loss of inhibition at low calcium would lead to hypercontractility (ie, increased population of force-generating states) and create a predisposition toward myocardial stiffness and ultimately diastolic dysfunction.

Next, we examined the effects of $TNNT2^{R94C}$ on the closed, open, and myosin-bound states of the thin filament (Figure 4A) by performing steady-state titrations of myosin binding to reconstituted pyrene-labeled thin filaments at high (pCa 3), low (2 mmol/L of EGTA), and intermediate calcium concentrations (pCa 6.25)[32,44] (Figure 4C and 4D). Qualitatively, the myosin binding isotherms for the $TNNT2^{WT}$ and $TNNT2^{R94C}$ thin filaments are similar at high and intermediate calcium concentrations; however, at low calcium, myosin binding to $TNNT2^{R94C}$ thin filaments is increased at low myosin concentrations compared with $TNNT2^{WT}$. These findings are consistent with the stopped flow data showing less inhibition to myosin binding at low calcium. Fitting of the data (see Table S1 for details) demonstrates that $TNNT2^{R94C}$ has an increased equilibrium constant for myosin weak binding, K_W (0.20 −0.03/+0.16 for $TNNT2^{R94C}$ versus 0.13 −0.01/+0.01 for the WT; P=0.002). The variant does not significantly change the equilibrium constant between the closed and open states. This includes K_T, (0.11 [−0.08, 0.12] for $TNNT2^{R94C}$ versus 0.06 [−0.03, 0.06] for the WT at low calcium, P=0.43; 0.07 [−0.04, 0.05] for $TNNT2^{R94C}$ versus 0.08 [−0.04, 0.04] for the WT at intermediate calcium, P=0.45; and 0.14 [−0.08, 0.09] for $TNNT2^{R94C}$ versus 0.18 [−0.07, 0.08] for the WT at high calcium, P=0.37). Furthermore, cooperativity of activation was unchanged between $TNNT2^{R94C}$ versus $TNNT2^{WT}$, n (4.47 [−1.66, 2.18] for $TNNT2^{R94C}$ versus $TNNT2^{WT}$; P=0.18). These results are summarized in Figure 5A and 5B.

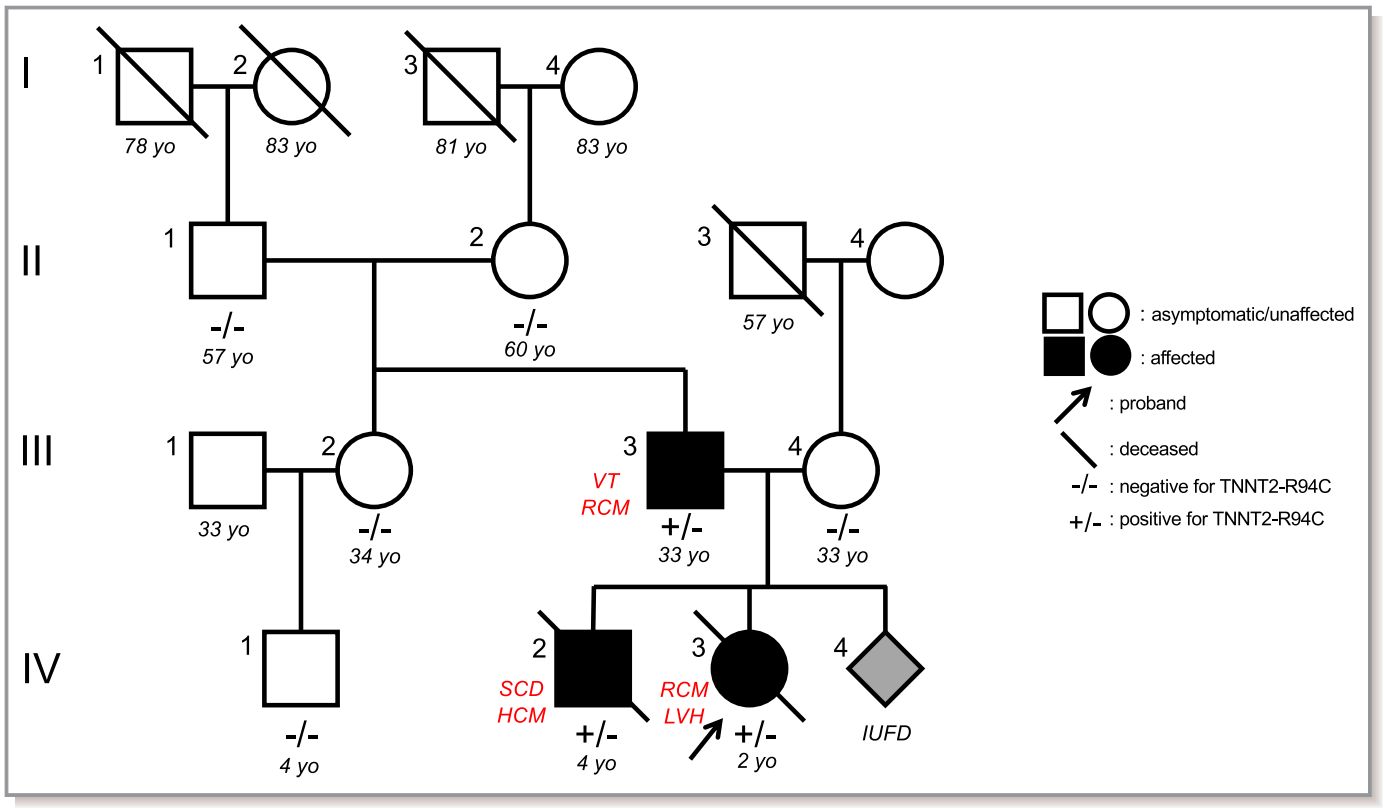

Figure 3. Pedigree of TNNT-R94C kindred. Four generations were evaluated (denoted by roman numerals). Clinical presentations are noted in red. The predominant phenotype is an RCM with mild hypertrophic features. Arrow denotes the proband (IV.4). Circles denote female, and squares denote male. Black fill denotes diagnosis of cardiomyopathy. Gray fill denotes fetal demise (IUFD). White fill denotes no cardiac diagnosis either following clinical evaluation or by reported history. +/− denotes heterozygosity for TNNT2-R94C variant whereas −/− denotes wild type. Diagonal line denotes deceased. HCM indicates hypertrophic cardiomyopathy; IUFD, intrauterine fetal demise; LVH, left ventricular hypertrophy; RCM, restrictive cardiomyopathy; SCD, sudden cardiac death; TNNT2, *TNNT2*-encoded cardiac troponin T; VT, ventricular tachycardia.

Computational Modeling Reveals Hypercontractility in TNNT2^{R94C}

These biochemical experiments identified the primary effects of TNNT2^{R94C} on thin filament regulation as 2-fold increases in the values for both K_B and K_W. Computational modeling was used to predict how these changes in equilibrium constants would affect the force-calcium curve in cardiac muscle.[46] Modeling demonstrates a shift in the force-pCa curve for TNNT2^{R94C} toward submaximal calcium activation compared with TNNT2^{WT}, consistent with molecular hypercontractility. The model also predicts that even at resting calcium concentrations (100–150 nmol/L[49,50]), there could be some basal level of activation with TNNT2^{R94C} (Figure 5C). Taken together, these data demonstrate that TNNT2^{R94C} would yield less calcium-induced inhibition to contraction, leading to hypercontractility and potentially an increase in basal muscle tension. These contractile defects could lead to diastolic dysfunction, culminating in restrictive cardiac physiology.

Table. In Silico Variant Prediction Aggregate Analysis of the TNNT2 Arg94Cys Variant Using Variant Prediction Models

Tool	Algorithm	Clinical Significance	Confidence (%)
GenMAPP	Pathway analysis tool	Deleterious	72
PolyPhen-2	Naïve Bayes classification	Deleterious	81
PredictSNP	Metaserver	Deleterious	76
SIFT	Sequence conservation	Deleterious	79
SNAP	Neural networks	Neutral	50
PANTHER	Ontology association	Deleterious	65

GenMAPP indicates gene map annotator and pathway profiler; PANTHER, protein analysis through evolutionary relationships; PolyPhen-2, polymorphism phenotyping v2; SIFT, sorting intolerant from tolerant.

Discussion

Spectrum of Cardiomyopathy Phenotypic Presentation

Recent advances in high-throughput sequencing have facilitated the identification of a number of novel cardiomyopathy-

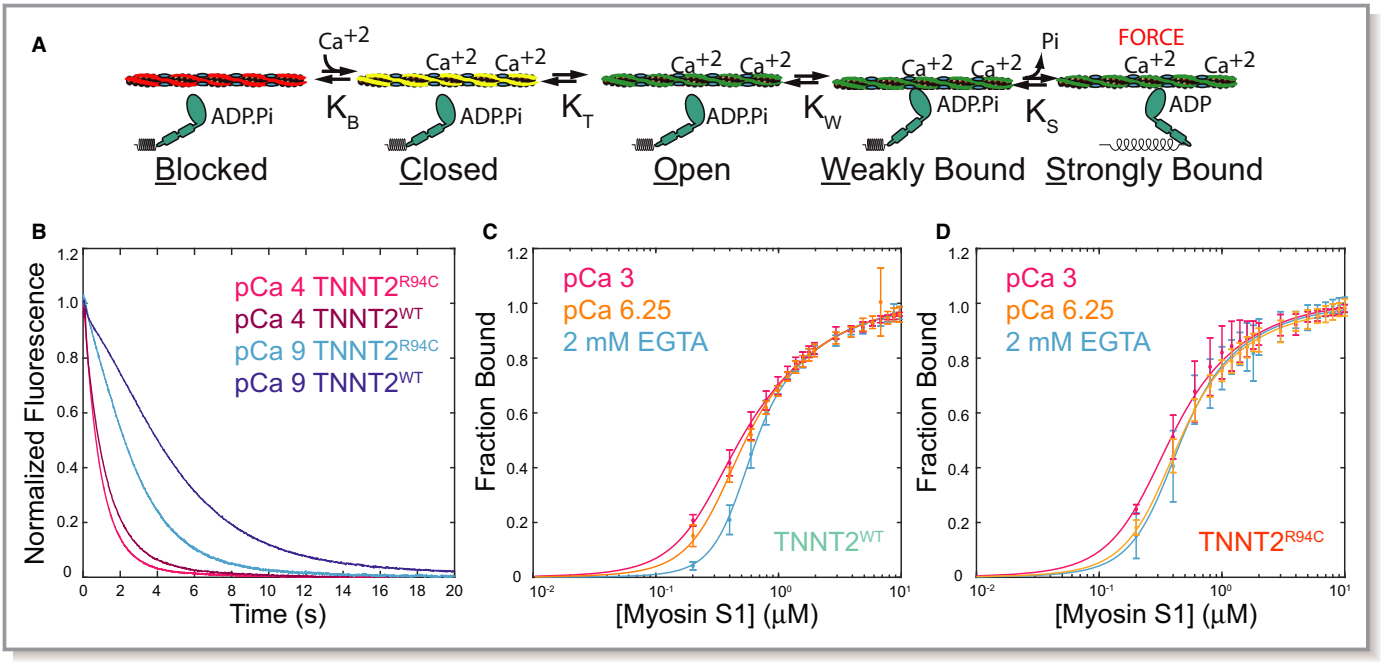

Figure 4. Measurement of the biochemical steps involved in thin filament activation. (**A**) Kinetic scheme for thin filament activation. Tropomyosin lies along the thin filament in 3 positions: blocked (red), closed (yellow), and open (green). Positioning of tropomyosin depends both on calcium and myosin binding. Myosin binds weakly to the thin filament before undergoing an isomerization to the strong-binding state, where force is generated. (**B**) Measurement of K_B, the equilibrium constant between the blocked and closed states, was measured by rapidly mixing myosin with pyrene-labeled thin filaments at low (pCa 9) and high calcium (pCa 4). Myosin binding quenches fluorescence. The ratio of the rates of binding at high and low calcium can be used to calculate K_B (see Methods). There is significantly less blocking in the R94C mutant than the WT at low calcium, as evidenced by the faster binding of the mutant at low calcium. (**C** and **D**) Equilibrium titrations of myosin with pyrene-labeled regulated thin filaments enable the calculation of several equilibrium constants (see Methods). Experiments were conducted with thin filaments containing either (**C**) TNNT2^{WT} or (**D**) TNNT2^{R94C}. TNNT2 indicates *TNNT2*-encoded cardiac troponin T.

associated genes, with the number identified as pathogenic increasing significantly over the last few years.[9] Because of the increased utilization of this technology, it is now possible to identify shared genetic variants among phenotypically dissimilar individuals, whose clinical presentations have not previously been associated with specific genes.[51] This has increased understanding of the role of genetic variants in the predisposing pathophysiological mechanisms of atypical forms of cardiomyopathy.[52] Here, we describe a variant associated with relatively mild hypertrophy and clear evidence of restrictive physiology consistent with RCM. It is well established that cardiomyopathic diseases, including RCM, have variable expressivity of disease frequently yielding a wide spectrum of phenotypes.[53,54] This study is supportive of these previous findings.

We report on a family in which a single variant in *TNNT2* is associated with restrictive cardiomyopathy and sudden cardiac death. The TNNT2-R94C variant was not observed in control populations and was predicted to be deleterious by in silico modeling, ClinVar, and current American College of Medical Genetics guidelines. Our biochemical data show a clear molecular phenotype that would be consistent with hypercontractility and diastolic dysfunction, supporting the concept that this variant is causative for the disease. There are a total of 5 previous reports of the TNNT2-R94C variant (National Center for Biotechnology Information ClinVar database), all with the designation of "pathogenic" or "likely pathogenic" and associated with familial HCM.[13,55–58] There has only been 1 previous report of a *TNNT2* variant causing restrictive physiology by autosomal-dominant inheritance.[13] Although the TNNT2-R94C variant has been previously associated with HCM, the spectrum of phenotypic features associated with TNNT2-R94C, including RCM, has not been well described.

Contractile Defects Caused by the R94C Variant

Overall, the clinical phenotype of RCM consists of severe diastolic dysfunction leading to atrial enlargement and, at most, mild ventricular hypertrophy. The molecular mechanisms of contractile defects causing diastolic disease remain largely unknown. Reflecting this, genetic causes of pediatric RCM cases remain unexplained, with only rare patients hosting variants within the thin filament. Here, we put forward TNNT2-R94C as a likely causative of disease. TNNT2 is part of the troponin complex that regulates calcium-dependent interactions between the molecular motor myosin and thin

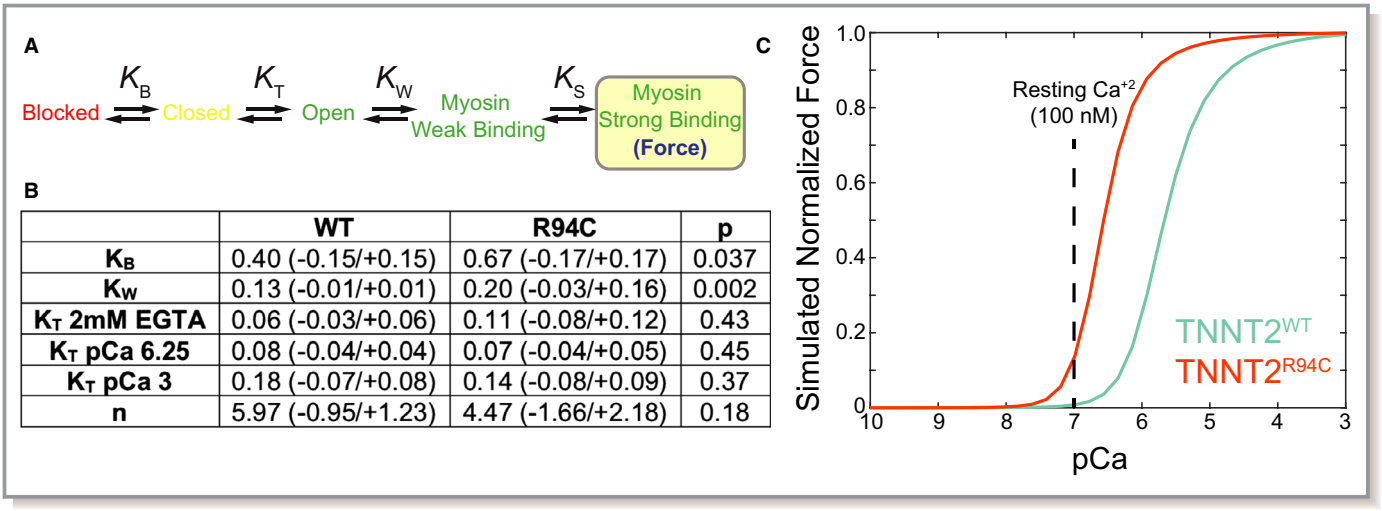

	WT	R94C	p
K_B	0.40 (-0.15/+0.15)	0.67 (-0.17/+0.17)	0.037
K_W	0.13 (-0.01/+0.01)	0.20 (-0.03/+0.16)	0.002
K_T 2mM EGTA	0.06 (-0.03/+0.06)	0.11 (-0.08/+0.12)	0.43
K_T pCa 6.25	0.08 (-0.04/+0.04)	0.07 (-0.04/+0.05)	0.45
K_T pCa 3	0.18 (-0.07/+0.08)	0.14 (-0.08/+0.09)	0.37
n	5.97 (-0.95/+1.23)	4.47 (-1.66/+2.18)	0.18

Figure 5. (**A**) Simplified kinetic scheme for thin filament activation. (**B**) Equilibrium constants measured for the thin filaments containing TNNT2^{WT} and TNNT2^{R94C}. The mutant causes statistically significant increases in K_B and K_W. (**C**) Computational modeling of the effects of the variant on the force-calcium relationship. The variant causes a leftward shift in the curve, signifying hypercontractility at lower calcium and a basal level of tension, even at resting calcium concentrations. K_B indicates the equilibrium constant between the blocked and closed states; K_W, the equilibrium constant between the closed and open states; TNNT2, *TNNT2*-encoded cardiac troponin T; WT, wild type.

filament. R94 is located in the highly conserved region of the TNNT2 N-terminal segment, and it is located near other residues that have been associated with other forms of cardiomyopathy, such as R92.[59–64] Currently, there is no high-resolution molecular structure of the thin filament or this region of TNNT2, so it is not possible to determine the exact structural basis of the biophysical changes that we observe; however, it has been proposed that this region plays an important role in mediating interaction between tropomyosin and the troponin complex. HCM variants in this region have been associated with reduced affinity of troponin for tropomyosin,[65,66] leading to the proposal that variant-induced changes in this affinity could reduce the ability of troponin to regulate interactions between myosin and the thin filament.[65] Our data, showing destabilization of the blocked state, would be consistent with this concept.

Previous analyses of the biochemical effects of HCM-associated TNNT2 mutations at the R94 position have demonstrated that appropriate calcium regulation is critical to normal function of the troponin complex.[18,19] Based on these findings, calcium sensitization is hypothesized to have a direct impact on cardiac systolic function, with calcium desensitization likely leading to decreased systolic function and calcium sensitization likely leading to increased systolic function. The described R94C variant is novel in that it produces a clinical phenotype of RCM and primarily diastolic dysfunction, making it an optimal variant for biochemical studies to investigate the interaction between calcium sensitivity and diastolic dysfunction.

Our computational modeling predicts that the R94C variant will lead to submaximal calcium activation and possibly an increase in basal tension during diastole. Previous studies of many HCM variants have demonstrated similar shifts toward submaximal calcium activation, leading to the proposal that these variants cause net hypercontractility and diastolic dysfunction. The phenotype observed in R94C patients, consisting of a primarily restrictive phenotype with mild hypertrophy, would be consistent with this hypothesis.

Limitations

Although we illustrate a novel genetic cause of RCM, our findings are based around a single family and may limit study generalizability. Our classification of this variant as causative for the disease is supported by our biochemical studies demonstrating that the introduction of this single point variant alone causes hypercontractility and features of diastolic dysfunction at the molecular scale. Further studies are warranted to determine how the findings presented here translate to cellular and organ levels; however, our study clearly identifies the initial lesion that leads to downstream changes with disease progression. Clinical genetic testing for patients with cardiomyopathic disease is routinely limited to genes of the sarcomere and metabolism, which are known causes of cardiomyopathy. It is possible that another variant or variants may be contributing to the severe phenotype observed in the family. This is unlikely, considering that the results of our biochemical experiments clearly demonstrate a pathological mechanism of disease.

Moreover, caution should be used when extrapolating the results here to the disease progression observed in human patients. Our biochemical experiments and modeling were

performed using all mutant troponin; however, most patients with the disease are heterozygous for the variant, and the exact proportion of protein that is expressed and incorporated into the sarcomere can vary with the variant. Moreover, as the disease progresses, there are changes in gene expression, fibrosis, and cellular organization that occur over the course of years. Although our modeling cannot capture the full complexity of the disease progression, it clearly demonstrates the initial contractile defects that lead to the disease phenotype. Future studies will be needed to identify the connection between the initial defect and disease phenotype observed in patients in the later stages of the disease.

Conclusions

The R94C variant in TNNT2 is a novel genetic cause of RCM occurring in a conserved domain which causes dysfunction of calcium-based regulation of cardiac contraction and likely yields significant myocardial diastolic dysfunction. This variant, when compared with control cohorts, has a high likelihood of producing a malignant phenotype. Furthermore, this work demonstrates the power of using in vitro biochemical studies as well as computational modeling to support disease causality.

Acknowledgments

We acknowledge Lina Greenberg for technical support in generating and purifying the mutant proteins.

Sources of Funding

Ezekian is supported by the NIH Clinical and Translational Science Award (UL1TR00255). Clippinger is supported by the NIH (T32EB018266). Greenberg is supported by the NIH (R01HL141086), the March of Dimes Foundation (FY18-BOC-430198), and the Children's Discovery Institute of Washington University and St. Louis Children's Hospital (PM-LI-2019-829). Landstrom is supported by the Phoebe Muzzy-McCrae Foundation and Duke University School of Medicine.

Disclosures

None.

References

1. Elliott P, Andersson B, Arbustini E, Bilinska Z, Cecchi F, Charron P, Dubourg O, Kuhl U, Maisch B, McKenna WJ, Monserrat L, Pankuweit S, Rapezzi C, Seferovic P, Tavazzi L, Keren A. Classification of the cardiomyopathies: a position statement from the European Society Of Cardiology Working Group on Myocardial and Pericardial Diseases. *Eur Heart J*. 2008;29:270–276.
2. Anderson HN, Cetta F, Driscoll DJ, Olson TM, Ackerman MJ, Johnson JN. Idiopathic restrictive cardiomyopathy in children and young adults. *Am J Cardiol*. 2018;121:1266–1270.
3. Cetta F, O'Leary PW, Seward JB, Driscoll DJ. Idiopathic restrictive cardiomyopathy in childhood: diagnostic features and clinical course. *Mayo Clin Proc*. 1995;70:634–640.
4. Harvey PA, Leinwand LA. The cell biology of disease: cellular mechanisms of cardiomyopathy. *J Cell Biol*. 2011;194:355–365.
5. Maron BJ, Haas TS, Ahluwalia A, Murphy CJ, Garberich RF. Demographics and epidemiology of sudden deaths in young competitive athletes: from the United States National Registry. *Am J Med*. 2016;129:1170–1177.
6. Maron MS, Hellawell JL, Lucove JC, Farzaneh-Far R, Olivotto I. Occurrence of clinically diagnosed hypertrophic cardiomyopathy in the United States. *Am J Cardiol*. 2016;117:1651–1654.
7. Van Driest SL, Ommen SR, Tajik AJ, Gersh BJ, Ackerman MJ. Sarcomeric genotyping in hypertrophic cardiomyopathy. *Mayo Clin Proc*. 2005;80:463–469.
8. Watkins H, Ashrafian H, Redwood C. Inherited cardiomyopathies. *N Engl J Med*. 2011;364:1643–1656.
9. Sabater-Molina M, Perez-Sanchez I, Hernandez Del Rincon JP, Gimeno JR. Genetics of hypertrophic cardiomyopathy: a review of current state. *Clin Genet*. 2018;93:3–14.
10. Wang L, Kim K, Parikh S, Cadar AG, Bersell KR, He H, Pinto JR, Kryshtal DO, Knollmann BC. Hypertrophic cardiomyopathy-linked mutation in troponin T causes myofibrillar disarray and pro-arrhythmic action potential changes in human iPSC cardiomyocytes. *J Mol Cell Cardiol*. 2018;114:320–327.
11. Wang L, Kryshtal DO, Kim K, Parikh S, Cadar AG, Bersell KR, He H, Pinto JR, Knollmann BC. Myofilament calcium-buffering dependent action potential triangulation in human-induced pluripotent stem cell model of hypertrophic cardiomyopathy. *J Am Coll Cardiol*. 2017;70:2600–2602.
12. Baudenbacher F, Schober T, Renato Pinto J, Sidorov VY, Hilliard F, Solaro RJ, Potter JD, Knollmann BC. Myofilament Ca^{2+} sensitization causes susceptibility to cardiac arrhythmia in mice. *J Clin Invest*. 2008;118:3893–3903.
13. Varnava A, Baboonian C, Davison F, de Cruz L, Elliott PM, Davies MJ, McKenna WJ. A new mutation of the cardiac troponin T gene causing familial hypertrophic cardiomyopathy without left ventricular hypertrophy. *Heart*. 1999;82:621–624.
14. Parvatiyar MS, Pinto JR. Pathogenesis associated with a restrictive cardiomyopathy mutant in cardiac troponin T is due to reduced protein stability and greatly increased myofilament Ca^{2+} sensitivity. *Biochim Biophys Acta*. 2015;1850:365–372.
15. Kaski JP, Syrris P, Burch M, Tome-Esteban MT, Fenton M, Christiansen M, Andersen PS, Sebire N, Ashworth M, Deanfield JE, McKenna WJ, Elliott PM. Idiopathic restrictive cardiomyopathy in children is caused by mutations in cardiac sarcomere protein genes. *Heart*. 2008;94:1478–1484.
16. Gallego-Delgado M, Delgado JF, Brossa-Loidi V, Palomo J, Marzoa-Rivas R, Perez-Villa F, Salazar-Mendiguchia J, Ruiz-Cano MJ, Gonzalez-Lopez E, Padron-Barthe L, Bornstein B, Alonso-Pulpon L, Garcia-Pavia P. Idiopathic restrictive cardiomyopathy is primarily a genetic disease. *J Am Coll Cardiol*. 2016;67:3021–3023.
17. Menon SC, Michels VV, Pellikka PA, Ballew JD, Karst ML, Herron KJ, Nelson SM, Rodeheffer RJ, Olson TM. Cardiac troponin T mutation in familial cardiomyopathy with variable remodeling and restrictive physiology. *Clin Genet*. 2008;74:445–454.
18. Lu QW, Morimoto S, Harada K, Du CK, Takahashi-Yanaga F, Miwa Y, Sasaguri T, Ohtsuki I. Cardiac troponin T mutation R141W found in dilated cardiomyopathy stabilizes the troponin T-tropomyosin interaction and causes a Ca^{2+} desensitization. *J Mol Cell Cardiol*. 2003;35:1421–1427.
19. Mickelson AV, Chandra M. Hypertrophic cardiomyopathy mutation in cardiac troponin T (R95H) attenuates length-dependent activation in guinea pig cardiac muscle fibers. *Am J Physiol Heart Circ Physiol*. 2017;313:H1180–H1189.
20. Lek M, Karczewski KJ, Minikel EV, Samocha KE, Banks E, Fennell T, O'Donnell-Luria AH, Ware JS, Hill AJ, Cummings BB, Tukiainen T, Birnbaum DP, Kosmicki JA, Duncan LE, Estrada K, Zhao F, Zou J, Pierce-Hoffman E, Berghout J, Cooper DN, Deflaux N, DePristo M, Do R, Flannick J, Fromer M, Gauthier L, Goldstein J, Gupta N, Howrigan D, Kiezun A, Kurki MI, Moonshine AL, Natarajan P, Orozco L, Peloso GM, Poplin R, Rivas MA, Ruano-Rubio V, Rose SA, Ruderfer DM, Shakir K, Stenson PD, Stevens C, Thomas BP, Tiao G, Tusie-Luna MT, Weisburd B, Won HH, Yu D, Altshuler DM, Ardissino D, Boehnke M, Danesh J, Donnelly S, Elosua R, Florez JC, Gabriel SB, Getz G, Glatt SJ, Hultman CM, Kathiresan S, Laakso M, McCarroll S, McCarthy MI, McGovern D, McPherson R, Neale BM, Palotie A, Purcell SM, Saleheen D, Scharf JM, Sklar P, Sullivan PF, Tuomilehto J, Tsuang MT, Watkins HC, Wilson JG, Daly MJ, MacArthur DG; Exome Aggregation Consortium. Analysis of protein-coding genetic variation in 60,706 humans. *Nature*. 2016;536:285–291.
21. Richards S, Aziz N, Bale S, Bick D, Das S, Gastier-Foster J, Grody WW, Hegde M, Lyon E, Spector E, Voelkerding K, Rehm HL; ACMG Laboratory Quality Assurance Committee. Standards and guidelines for the interpretation of

sequence variants: a joint consensus recommendation of the American College of Medical Genetics and Genomics and the Association for Molecular Pathology. *Genet Med*. 2015;17:405–424.

22. Landrum MJ, Lee JM, Benson M, Brown GR, Chao C, Chitipiralla S, Gu B, Hart J, Hoffman D, Jang W, Karapetyan K, Katz K, Liu C, Maddipatla Z, Malheiro A, McDaniel K, Ovetsky M, Riley G, Zhou G, Holmes JB, Kattman BL, Maglott DR. ClinVar: improving access to variant interpretations and supporting evidence. *Nucleic Acids Res*. 2018;46:D1062–D1067.
23. NCBI. Troponin T, cardiac muscle isoform 2 [Homo sapiens]. 2019:NCBI Reference Sequence: NP_001001430.1. Bethesda MD: National Center for Biotechnology Information.
24. Corpet F. Multiple sequence alignment with heirarchical clustering. *Nucleic Acids Res*. 1988;16:10881–10890.
25. Corpet F, Gouzy J, Kahn D. Browsing protein families via the 'Rich Family Description' format. *Bioinformatics*. 1999;15:1020–1027.
26. Dahlquist KD, Salomonis N, Vranizan K, Lawlor SC, Conklin BR. GenMAPP, a new tool for viewing and analyzing microarray data on biological pathways. *Nat Genet*. 2002;31:19–20.
27. Adzhubei IA, Schmidt S, Peshkin L, Ramensky VE, Gerasimova A, Bork P, Kondrashov AS, Sunyaev SR. A method and server for predicting damaging missense mutations. *Nat Methods*. 2010;7:248–249.
28. Bendl J, Stourac J, Salanda O, Pavelka A, Wieben ED, Zendulka J, Brezovsky J, Damborsky J. PredictSNP: robust and accurate consensus classifier for prediction of disease-related mutations. *PLoS Comput Biol*. 2014;10:e1003440.
29. Sim NL, Kumar P, Hu J, Henikoff S, Schneider G, Ng PC. SIFT web server: predicting effects of amino acid substitutions on proteins. *Nucleic Acids Res*. 2012;40:W452–W457.
30. Korf I. Gene finding in novel genomes. *BMC Bioinformatics*. 2004;5:59.
31. Mi H, Muruganujan A, Ebert D, Huang X, Thomas PD. PANTHER version 14: more genomes, a new PANTHER GO-slim and improvements in enrichment analysis tools. *Nucleic Acids Res*. 2019;47:D419–D426.
32. Barrick SK, Clippinger SR, Greenberg L, Greenberg MJ. Computational tool to study perturbations in muscle regulation and its application to heart disease. *Biophys J*. 2019;116:2246–2252.
33. Clippinger SR, Cloonan PE, Greenberg L, Ernst M, Stump WT, Greenberg MJ. Disrupted mechanobiology links the molecular and cellular phenotypes in familial dilated cardiomyopathy. *Proc Natl Acad Sci USA*. 2019;116:17831–17840.
34. Greenberg MJ, Shuman H, Ostap EM. Inherent force-dependent properties of beta-cardiac myosin contribute to the force-velocity relationship of cardiac muscle. *Biophys J*. 2014;107:L41–L44.
35. Eads TM, Thomas DD, Austin RH. Microsecond rotational motions of eosin-labeled myosin measured by time-resolved anisotropy of absorption and phosphorescence. *J Mol Biol*. 1984;179:55–81.
36. Margossian SS, Lowey S. Preparation of myosin and its subfragments from rabbit skeletal muscle. *Methods Enzymol*. 1982;85(Pt B):55–71.
37. Spudich JA, Watt S. The regulation of rabbit skeletal muscle contraction. I. Biochemical studies of the interaction of the tropomyosin-troponin complex with actin and the proteolytic fragments of myosin. *J Biol Chem*. 1971;246:4866–4871.
38. Pollard TD. Purification of a high molecular weight actin filament gelation protein from Acanthamoeba that shares antigenic determinants with vertebrate spectrins. *J Cell Biol*. 1984;99:1970–1980.
39. Greenberg MJ, Lin T, Goldman YE, Shuman H, Ostap EM. Myosin IC generates power over a range of loads via a new tension-sensing mechanism. *Proc Natl Acad Sci USA*. 2012;109:E2433–E2440.
40. Hitchcock-DeGregori SE, Heald RW. Altered actin and troponin binding of amino-terminal variants of chicken striated muscle alpha-tropomyosin expressed in *Escherichia coli*. *J Biol Chem*. 1987;262:9730–9735.
41. Pan S, Sommese RF, Sallam KI, Nag S, Sutton S, Miller SM, Spudich JA, Ruppel KM, Ashley EA. Establishing disease causality for a novel gene variant in familial dilated cardiomyopathy using a functional in-vitro assay of regulated thin filaments and human cardiac myosin. *BMC Med Genet*. 2015;16:97.
42. McIntosh BB, Holzbaur EL, Ostap EM. Control of the initiation and termination of kinesin-1-driven transport by myosin-Ic and nonmuscle tropomyosin. *Curr Biol*. 2015;25:523–529.
43. Kozaili JM, Leek D, Tobacman LS. Dual regulatory functions of the thin filament revealed by replacement of the troponin I inhibitory peptide with a linker. *J Biol Chem*. 2010;285:38034–38041.
44. McKillop DF, Geeves MA. Regulation of the interaction between actin and myosin subfragment 1: evidence for three states of the thin filament. *Biophys J*. 1993;65:693–701.
45. Maytum R, Westerdorf B, Jaquet K, Geeves MA. Differential regulation of the actomyosin interaction by skeletal and cardiac troponin isoforms. *J Biol Chem*. 2003;278:6696–6701.
46. Campbell SG, Lionetti FV, Campbell KS, McCulloch AD. Coupling of adjacent tropomyosins enhances cross-bridge-mediated cooperative activation in a Markov model of the cardiac thin filament. *Biophys J*. 2010;98:2254–2264.
47. Colan S. Normal echocardiographic values for cardiovascular structures. In: Lai W, Cohen M, Geva T, Mertens L, eds. *Echocardiography in Pediatric and Congenital Heart Disease*. West Sussex, UK: Wiley-Blackwell; 2009:765–785.
48. Molina DK, Pinneri K, Stash JA, Li L, Vance K, Cross C. Organ weight reference ranges for ages 0 to 12 years. *Am J Forensic Med Pathol*. 2019;40:318–328.
49. Guatimosim S, Dilly K, Santana LF, Saleet Jafri M, Sobie EA, Lederer WJ. Local Ca(2+) signaling and EC coupling in heart: Ca(2+) sparks and the regulation of the [Ca(2+)](i) transient. *J Mol Cell Cardiol*. 2002;34:941–950.
50. Bers DM. Cardiac excitation-contraction coupling. *Nature*. 2002;415:198–205.
51. Landstrom AP, Boczek NJ, Ye D, Miyake CY, De la Uz CM, Allen HD, Ackerman MJ, Kim JJ. Novel long QT syndrome-associated missense mutation, L762F, in CACNA1C-encoded L-type calcium channel imparts a slower inactivation tau and increased sustained and window current. *Int J Cardiol*. 2016;220:290–298.
52. Connell PS, Jeewa A, Kearney DL, Tunuguntla H, Denfield SW, Allen HD, Landstrom AP. A 14-year-old in heart failure with multiple cardiomyopathy variants illustrates a role for signal-to-noise analysis in gene test re-interpretation. *Clin Case Rep*. 2019;7:211–217.
53. Ho CY, Charron P, Richard P, Girolami F, Van Spaendonck-Zwarts KY, Pinto Y. Genetic advances in sarcomeric cardiomyopathies: state of the art. *Cardiovasc Res*. 2015;105:397–408.
54. Rindler TN, Hinton RB, Salomonis N, Ware SM. Molecular characterization of pediatric restrictive cardiomyopathy from integrative genomics. *Sci Rep*. 2017;7:39276.
55. Lopes LR, Syrris P, Guttmann OP, O'Mahony C, Tang HC, Dalageorgou C, Jenkins S, Hubank M, Monserrat L, McKenna WJ, Plagnol V, Elliott PM. Novel genotype-phenotype associations demonstrated by high-throughput sequencing in patients with hypertrophic cardiomyopathy. *Heart*. 2015;101:294–301.
56. Berge KE, Leren TP. Genetics of hypertrophic cardiomyopathy in Norway. *Clin Genet*. 2014;86:355–360.
57. Liu W, Liu W, Hu D, Zhu T, Ma Z, Yang J, Xie W, Li C, Li L, Yang J, Li T, Bian H, Tong Q. Mutation spectrum in a large cohort of unrelated Chinese patients with hypertrophic cardiomyopathy. *Am J Cardiol*. 2013;112:585–589.
58. Otsuka H, Arimura T, Abe T, Kawai H, Aizawa Y, Kubo T, Kitaoka H, Nakamura H, Nakamura K, Okamoto H, Ichida F, Ayusawa M, Nunoda S, Isobe M, Matsuzaki M, Doi YL, Fukuda K, Sasaoka T, Izumi T, Ashizawa N, Kimura A. Prevalence and distribution of sarcomeric gene mutations in Japanese patients with familial hypertrophic cardiomyopathy. *Circ J*. 2012;76:453-461.
59. Chandra M, Tschirgi ML, Tardiff JC. Increase in tension-dependent ATP consumption induced by cardiac troponin T mutation. *Am J Physiol Heart Circ Physiol*. 2005;289:H2112–H2119.
60. Ford SJ, Mamidi R, Jimenez J, Tardiff JC, Chandra M. Effects of R92 mutations in mouse cardiac troponin T are influenced by changes in myosin heavy chain isoform. *J Mol Cell Cardiol*. 2012;53:542–551.
61. Robinson P, Mirza M, Knott A, Abdulrazzak H, Willott R, Marston S, Watkins H, Redwood C. Alterations in thin filament regulation induced by a human cardiac troponin T mutant that causes dilated cardiomyopathy are distinct from those induced by troponin T mutants that cause hypertrophic cardiomyopathy. *J Biol Chem*. 2002;277:40710–40716.
62. Szczesna D, Zhang R, Zhao J, Jones M, Guzman G, Potter JD. Altered regulation of cardiac muscle contraction by troponin T mutations that cause familial hypertrophic cardiomyopathy. *J Biol Chem*. 2000;275:624–630.
63. Tobacman LS, Lin D, Butters C, Landis C, Back N, Pavlov D, Homsher E. Functional consequences of troponin T mutations found in hypertrophic cardiomyopathy. *J Biol Chem*. 1999;274:28363–28370.
64. Williams MR, Lehman SJ, Tardiff JC, Schwartz SD. Atomic resolution probe for allostery in the regulatory thin filament. *Proc Natl Acad Sci USA*. 2016;113:3257–3262.
65. Gangadharan B, Sunitha MS, Mukherjee S, Chowdhury RR, Haque F, Sekar N, Sowdhamini R, Spudich JA, Mercer JA. Molecular mechanisms and structural features of cardiomyopathy-causing troponin T mutants in the tropomyosin overlap region. *Proc Natl Acad Sci USA*. 2017;114:11115–11120.
66. Palm T, Graboski S, Hitchcock-DeGregori SE, Greenfield NJ. Disease-causing mutations in cardiac troponin T: identification of a critical tropomyosin-binding region. *Biophys J*. 2001;81:2827–2837.

SUPPLEMENTAL MATERIAL

Table S1. Clinical and genetic information for the multi-generational family.

Individual	Age (years)	Sex	Status	TNNT2-R94C Status	Cardiovascular Phenotype
I.1	78	M	Deceased	Unknown	
I.2	83	F	Deceased	Unknown	
I.3	81	M	Deceased	Unknown	
I.4	83	F	Alive	Unknown	
II.1	59	M	Alive	-/-	Atrial fibrillation
II.2	60	F	Alive	-/-	
II.3	57	M	Deceased	Unknown	
II.4	Unknown	F	Alive	Unknown	
III.1	33	M	Alive	Unknown	
III.2	31	F	Alive	-/-	Supraventricular tachycardia
III.3	35	M	Alive	+/-	Ventricular tachycardia
III.4	36	F	Alive	-/-	
IV.1	4	M	Alive	-/-	
IV.2	4	M	Deceased	+/-	Hypertrophic cardiomyopathy with restrictive features, sudden cardiac arrest
IV.3	2	F	Deceased	+/-	Restrictive cardiomyopathy with mild hypertrophy, sudden cardiac arrest
IV.4	Fetus	Unknown	Deceased	Unknown	First trimester fetal death